

Enhancing the Detection of Coronary Artery Disease Using Machine Learning

Karan Kumar Singh

Department of Computer Science and Engineering
Sharda University, Greater Noida, India
karankumarsingh7870@gmail.com

Nikita Gajbhiye

Department of Computer Science and Engineering
Sharda University, Greater Noida, India
nikitagajbhiye.ng@gmail.com

Gouri Sankar Mishra

Department of Computer Science and Engineering
Sharda University, Greater Noida, India
gourisankar.mishra@sharada.ac.in

March 10, 2026

Abstract

Coronary Artery Disease (CAD) remains a leading cause of morbidity and mortality worldwide. Early detection is critical to recover patient outcomes and decrease healthcare costs. In recent years, machine learning (ML) advancements have shown significant potential in enhancing the accuracy of CAD diagnosis. This study investigates the application of ML algorithms to improve the detection of CAD by analyzing patient data, including clinical features, imaging, and biomarker profiles. Bi-directional Long Short-Term Memory (Bi-LSTM), Gated Recurrent Units (GRU), and a hybrid of Bi-LSTM+GRU were trained on large datasets to predict the presence of CAD. Results demonstrated that these ML models outperformed traditional diagnostic methods in sensitivity and specificity, offering a robust tool for clinicians to make more informed decisions. The experimental results show that the hybrid model achieved an accuracy of 97.07%. By integrating advanced data preprocessing techniques and feature selection, this study ensures optimal learning and model performance, setting a benchmark for the

application of ML in CAD diagnosis. The integration of ML into CAD detection presents a promising avenue for personalized healthcare and could play a pivotal role in the future of cardiovascular disease management.

Keywords: Coronary Artery Disease, Deep Learning, Bi-LSTM, GRU, Hybrid Model

1 Introduction

Coronary Artery Disease (CAD*) occurs when the coronary arteries, which carry oxygen and nutrients to the heart muscle, are constricted or obstructed. Other names for this ailment include coronary and ischemic heart disease [1-3]. It is now well-recognized as an ongoing disease that poses the greatest risk to human life [4]. As per a recent study, the United States scores highest for both the prevalence of heart disease and the percentage of people diagnosed with the illness [5]. Many people suffer shortness of breath, swollen feet, extreme tiredness, and other signs of heart disease. CAD is the most prevalent form of Cardio Vascular Disease (CVD) and a leading cause of chest pain, stroke, and heart attacks. Heart rhythm problems, heart failure, congenital heart defects, and CVD are all forms of heart illness [6]. As a consequence, detecting CAD is essential for modern civilization. One of the most useful tools for diagnosing and guiding therapy for CAD is coronary angiography (CAG), which evaluates luminal stenosis, plaque features, and disease activity [7].

In healthcare applications, Machine Learning (ML) helps improve the diagnosis process and is therefore extensively used in medical science. To understand complicated and nonlinear patterns related to the characteristics, ML algorithms minimize the error between the projected and actual outcomes by analyzing data [13]. Integrating ML into medical applications has greatly improved diagnostic processes. ML has recently found several uses, assisting with nearly every aspect of medical diagnosis. These include cancer, Parkinson’s disease, thyroid illness, and several ocular ailments [14]. ML in the context of CAD diagnosis allows for the quick identification of CHD using Electrocardiograms (ECGs), Phonocardiograms (PCGs), Coronary Computed Tomography Angiography (CCTAs), and CAG [15]. A comprehensive overview of ML’s use in CAD diagnosis is provided in this paper. The research objective of the paper follows:

- To develop an ML model that can precisely predict the occurrence of

CAD using patient data such as demographic, clinical, and laboratory parameters.

- To compare the effectiveness of different ML algorithms (e.g., Decision Trees, Random Forest, Support Vector Machines, Neural Networks) for predicting CAD.
- To explore feature selection methods that identify the most significant predictors of CAD from a comprehensive dataset, ensuring that irrelevant variables do not hinder the model's accuracy.
- To enhance detection accuracy by incorporating advanced data pre-processing techniques, such as handling missing data, normalization, and outlier detection, to clean and optimize the dataset for better learning outcomes.

To validate the performance of the ML models using metrics such as Sensitivity, Specificity, Accuracy and area under the ROC curve (AUC) on training and unseen test datasets.

Machine learning techniques have been successfully applied in various healthcare and agricultural applications, including depression detection, kidney disease diagnosis, and plant disease classification, demonstrating their effectiveness in predictive analytics [14–16, 37].

2 Literature Review

In this section, the authors provide the previous work based on the detection of CAD using ML methods. All the results of previous work are evaluated in terms of Accuracy, Precision, Recall, Sensitivity, Specificity and F1-score. The performance metrics associated with the current approaches that are being evaluated are summarized in Table 1.

Table 1: Summary of the outcomes achieved by current ML-based approaches

Author [Reference]	Data Collection (No. of patients)	Methodology	Outcomes
Ma et al., [16]	Southwest China (300,000)	XG-Boost, RF, and LR	The AUC for the suggested model was 0.70.
Mijwil et al., [18]	UC Irvine ML repository (300)	MLP, RF, SVM, KNN, LR, NB, and DT	The MLP algorithm reached an accuracy of over 88%.
Hammoud et al., [19]	1190	LR, SVM, KNN, RF, DT, NB, and GB	The RF algorithm achieved the highest accuracy rates of 89.50% before tuning and 94.96% after tuning.
Asif et al., [20]	Heart disease dataset	RF, GB, and XG-Boost	The ensemble model attained remarkable results in terms of Sensitivity (96.37%), Accuracy (94.53%), and Precision (98.37%).
Lin et al., [21]	MIMIC-IV (5757)	Cat-Boost	The suggested model had the strongest predictive performance, with an AUC of 0.760 and a training set of 0.831.
Yilmaz et al., [22]	Heart Disease Dataset (11)	SVM and RF	The SVM model achieved Specificity of 0.844, Sensitivity of 0.971, NPV of 0.887, PPV of 0.976, and F1-score of 0.816.
Garavand et al., [23]	Z-Alizadeh Sani dataset (303)	MLP, SVM, LR, J48, RF, KNN, and NB	RF achieved the highest Accuracy (78.96%), Sensitivity (93.86%), Specificity (51.13%), MCC (0.5192), and ROC (0.8375).
Huang et al., [24]	Affiliated Hospital of Traditional Chinese Medicine of Southwest Medical University (2049)	RF, KNN, RBFNN, KRR, and SVM	RF achieved the highest Accuracy (78.96%), Sensitivity (93.86%), Specificity (51.13%), MCC

3 Methodology

Several recent studies have explored the use of machine learning and deep learning techniques for predictive modeling in healthcare and related domains. Previous works have demonstrated the effectiveness of optimized machine learning frameworks and hybrid deep learning architectures in solving complex classification problems [14–16, 37].

CAD is an important cause of mortality globally, requiring early detection and accurate diagnosis to prevent severe complications. Conventional diagnostic techniques, such as angiography, though accurate, are invasive and costly. Non-invasive diagnostic methods based on clinical data and medical images can potentially improve early detection, but their accuracy remains a challenge. The goal of this project is to develop a machine learning-based system to enhance the detection of CAD. By integrating an advanced Bi-LSTM algorithm, this project aims to build a robust system for CAD detection. This system will leverage clinical and imaging datasets to improve diagnostic accuracy and assist healthcare professionals in making informed decisions, thereby reducing the need for invasive procedures.

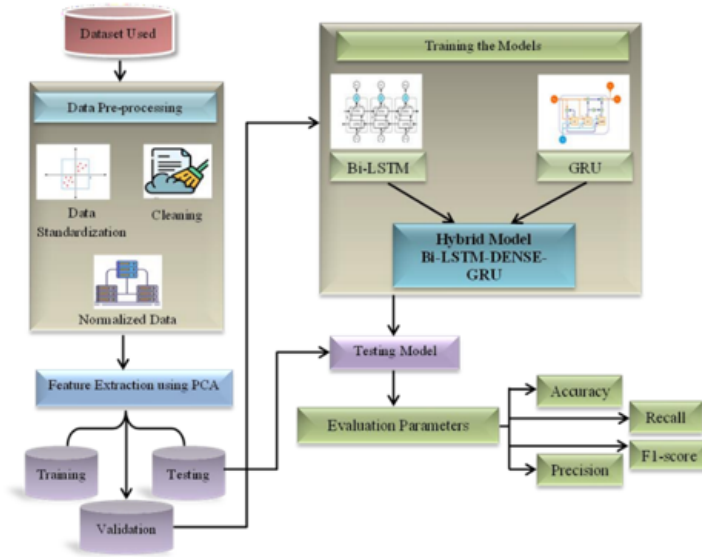


Figure 1: Block diagram of proposed methodology

3.1 Data Collection

A dataset of 1000 3D CCTA pictures has been created. A Siemens 128-slice dual- source scanner was used to collect the images. The images have a resolution of $512 \times 512 \times (206-275)$ voxels. The images were taken between 2012 and 2018 at the Shanti Hospital. On average, men were 67.68 years old, while females were 49.98 years old. Investigators can use the dataset repository [26] without restriction. Furthermore, it provides a way to segment images to get 3D views of coronary arteries.

3.2 Data Preprocessing

Pre-processing is a fundamental step in any ML workflow. It involves preparing the dataset for training by transforming raw data into an understandable format for models. Pre-processing can include data cleaning, data standardization, and data normalization.

Data Cleaning, sometimes known as data preparation, is an essential link in the data processing chain. The application of this method involves identifying and fixing any mistakes, inconsistencies, or missing values in the dataset. This is an essential step before doing any useful analysis of the dataset. In addition, the findings could be inflated, and the analysis might become confused if there are duplicate entries. This is achieved by removing the chance of accidental tampering, which helps ensure that the representational data is accurate [27].

Data Normalization is used to process the numeric data, which can avoid gradient dispersion, which is caused by the significant variance in individual features when employing the back-propagation technique [28]. A complicated dataset of features that DL struggles to extract is the consequence of not normalizing the data, which leads to a decline in gradient magnitude with back-propagation and a consequent slowing of the intrusion detection model’s update weight increase. The collected CCTA dataset was normalized using the z-score method. to $[-1, 1]$ using the z-score approach, as seen in Equation (1).

$$m'_i = \frac{m_i - \bar{m}}{x} \quad (1)$$

The values of the data sample before and after normalization are denoted by m_i and m'_i , respectively. The average value of the feature’s data before normalization is denoted by \bar{m} .

Data Standardization was used to transform the dataset from a normal distribution into a standard normal distribution because it contains charac-

teristics with varying ranges of values. Because of this, after rescaling, the mean value of an attribute is zero, and the standard deviation is the same as the distribution. The formula to compute a standard score (z-score) is:

$$z = \frac{x - \mu}{\sigma} \quad (2)$$

The data sample, the mean, and the standard deviation are represented by x , μ , and σ , respectively [29].

3.3 Feature Extraction

The strength and direction of the linear relationship between the two variables are measured by the coefficient of correlation, which can have values between -1 and 1. During the feature extraction process, the authors used the Pearson correlation matrix (PCM) [30] to determine which variables were most strongly connected. This allowed us to decrease the dataset’s dimensionality while keeping all of the crucial information. In the end, this allowed us to analyze the data more efficiently and effectively. The PCM, which it uses to find the most associated variables, can be utilized as well to spot any abnormalities or outliers in the dataset [31]. Optional feature extraction techniques like PCA or Independent Component Analysis (ICA) could be more suited when the variables’ relationships are not linear.

3.4 Classification Models

Bidirectional Long Short-Term Memory (Bi-LSTM) is an enhancement to the traditional LSTM that has been suggested to improve the performance of network models. For bidirectional (i.e., forward and backward) data processing, the Bi-LSTM model employs two hidden LSTM layers [32,33]. To do this, the main recursive layer of the neural model is duplicated. During training, the information that goes into the main layer is the real data, but the information that goes into the duplicate layer is the exact opposite. This strategy significantly enhances the quantity of data accessible to the model. The inner workings of a Bi-LSTM model. The Bi-LSTM forward hidden layer.

The Bi-LSTM forward hidden layer ($\vec{\beta}$), the backward hidden layer ($\overleftarrow{\beta}$), and the output (o) can be deduced from the following equations [34].

$$\vec{\beta}_t = f(W_{\beta}^{\rightarrow} x_t + U_{\beta}^{\rightarrow} \vec{\beta}_{t-1} + b^{\rightarrow}) \quad (3)$$

$$\overleftarrow{\beta}_t = f(W_\beta^\leftarrow x_t + U_\beta^\leftarrow \overleftarrow{\beta}_{t+1} + b^\leftarrow) \quad (4)$$

$$o_t = g(V_\beta[\overrightarrow{\beta}_t, \overleftarrow{\beta}_t] + c) \quad (5)$$

In this context, $\hat{W}_{\beta \rightarrow}^\alpha$ represents the backward hidden weight and $\hat{W}_{\rightarrow \beta}^\alpha$ represents the forward hidden weight. The term \mathfrak{h} refers to the hidden layer, whereas $\lambda_{\beta \rightarrow}$ and $\lambda_{\rightarrow \beta}$ denote the forward and backward bias vectors, respectively [35].

Gated Recurrent Unit (GRU) was created to tackle the issue of gradients that disappear or explode. It is an enhanced version of the LSTM model that also uses gate structures to regulate the flow of information. The absence of an output gate at GRU means that all data is accessible to the whole public, which is a significant observation [36]. GRUs only have two gates—one for updating and one for resetting—but LSTMs combine input and forget gates. The simplified structure of GRUs allows them to increase performance with fewer parameters. Following equations describe the GRU update and reset gates:

$$m_t = \sigma(W_m[h_{t-1}, x_t] + U_m h_{t-1} + b_m) \quad (6)$$

$$n_t = \sigma(W_n[h_{t-1}, x_t] + U_n h_{t-1} + b_n) \quad (7)$$

where m_t is the reset gate at time step t , n_t is the update gate at time step t , h_{t-1} is the hidden state at time step $t-1$, x_t is the input at time step t , W_m and W_n are the weight matrices for the reset and update gates, U_m and U_n are the weight matrices applied to the hidden state, b_m and b_n are the bias vectors for the reset and update gates, and σ denotes the sigmoid activation function. The candidate hidden state \tilde{h}_t is then computed as follows.

$$\tilde{h}_t = \tanh(W[m_t * h_{t-1}, x_t] + b) \quad (8)$$

The position of the carry gate $(1 - n_t)$ determines the extent to which the previous hidden state is carried forward, as well as the range of values through which the candidate hidden state is used to update the previous hidden state.

$$h_t = (1 - n_t)h_{t-1} + n_t\tilde{h}_t \quad (9)$$

3.5 Performance Metrics

The evaluation model consists of four components: TP, TN, FP, and FN. The term *True Positive* (TP) refers to the correct identification of a positive sample. Similarly, *True Negative* (TN) represents the correct prediction of a negative sample. When a positive sample is incorrectly predicted as negative, it is referred to as a *False Negative* (FN), whereas a *False Positive* (FP) occurs when a negative sample is incorrectly predicted as positive.

The performance of the model is evaluated using Equations (11)–(14), where Accuracy, F1-score, Precision, and Recall are the performance metrics. Accuracy is defined as the ratio of correctly predicted samples to the total number of predictions made by the model. The F1-score, also known as the harmonic mean of Precision and Recall, is used to measure the overall performance of the model. Recall measures the proportion of actual positive samples that are correctly identified by the model. Models with values closer to 1 generally indicate better performance according to the ROC curve.

$$Accuracy = \frac{TP + TN}{TP + TN + FP + FN} \quad (10)$$

$$Precision = \frac{TP}{TP + FP} \quad (11)$$

$$Recall = \frac{TP}{TP + FN} \quad (12)$$

$$F1\text{-score} = \frac{2 \times Precision \times Recall}{Precision + Recall} \quad (13)$$

4 Results and Analysis

4.1 Results of Bi-LSTM

The plot of Training Loss and Validation Loss over a series of epochs during the training of an ML model is shown in Fig. 2. The number of iterations or training cycles the model has gone through from 0 to around 30 epochs. The loss value measures how well the model is performing. A lower loss indicates a better model performance. The model initially starts with a higher loss (around 0.15) at epoch 1, but within the first few epochs (about 5), the training loss decreases sharply, indicating rapid learning. After epoch 5, the training loss continues to decrease but at a much slower rate, stabilizing at around 0.055. Like the training loss, the validation loss

also starts high, around 0.1, and quickly drops, nearly matching the training loss around epoch 5. After that, it follows a similar pattern, stabilizing slightly above the training loss (around 0.06). Both the training and validation losses are decreasing, indicating that the model is learning effectively without significant over-fitting.

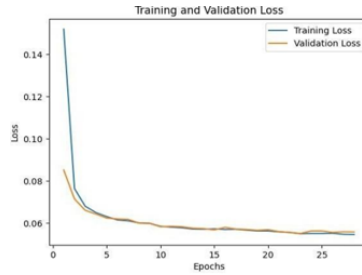


Figure 2: Training and validation loss of the Bi-LSTM model across epochs

The training and validation accuracy of a Bi-LSTM model across 30 epochs is shown in Fig. 3. The accuracy of the model is a measure of the proportion of correctly classified instances.

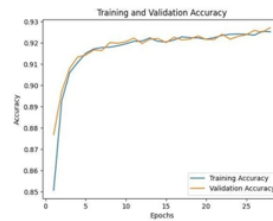


Figure 3: Training and validation accuracy of the Bi-LSTM model across epochs

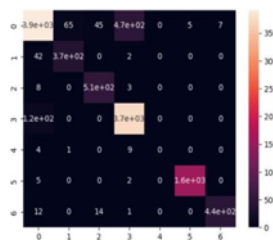


Figure 4: Confusion matrix of the Bi-LSTM model

The accuracy starts from around 85% (0.85) and rises to just above 92% (0.92). It starts at approximately 85% accuracy at epoch 1 and rises steeply in the first 5 epochs, reaching above 90%. After that, the training accuracy gradually increases and stabilizes around 92% to 93%, showing minimal fluctuation. It closely follows the training accuracy, starting slightly below the training accuracy but converging to a similar range between 92% and 93% after around 5 epochs. There are some slight fluctuations in validation accuracy, but overall, it remains close to the training accuracy.

Table 2 presents the evaluation results of the Bi-LSTM model, achieving an Accuracy of 92.7%, Precision of 92.9%, Recall of 92.7%, and an F1-score of 92.7%.

Table 2: Evaluation of Bi-LSTM

Parameters	Value (%)
Accuracy	92.7
Precision	92.9
Recall	92.7
F1-score	92.7

4.2 Results of GRU Model

Fig. 5 illustrates the training and validation loss over 25 epochs. Both losses start high, around 0.18, and decrease rapidly within the first few epochs, indicating that the model is learning effectively. By epoch 5, both training and validation losses converge near 0.06. After this point, the losses continue to gradually decrease and stabilize around 0.04 until epoch 20. Around epoch 20, there is a slight increase in both training and validation losses, which could signal slight overfitting or model instability, but the losses remain low overall. The model seems to generalize well, as the training and validation losses follow a similar trend and are closely aligned.

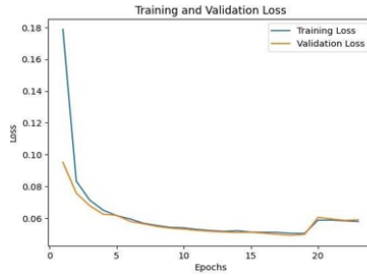


Figure 5: Training and validation loss of the GRU model across epochs

Fig. 6 shows the training and validation accuracy curves over 25 epochs for a GRU model. Both the training and validation accuracies start around 0.82 and improve significantly within the first 5 epochs. The training accuracy rises rapidly and stabilizes around 0.93, while the validation accuracy follows a similar trend but with more fluctuations. Around epoch 10, both accuracies converge near their peak (above 0.92), indicating good model performance. However, around epoch 20, there is a sudden drop in validation accuracy, possibly suggesting some over-fitting or instability in the model's generalization capability at this point. After the drop, the validation accuracy recovers slightly but remains below the earlier peak. Overall, the model performs well, with both accuracies stabilizing after initial training. Fig. 7 shows the confusion matrix of GRU model.

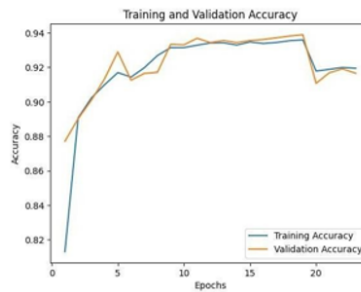


Figure 6: Training and validation accuracy of the GRU model across epochs

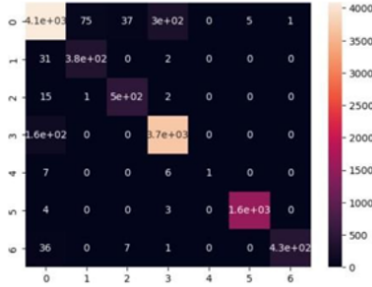


Figure 7: Confusion matrix of the GRU model

Table 3 provides the evaluation results of the GRU model, which achieved an Accuracy of 93.9%, Precision of 94.0%, Recall of 93.9%, and an F1-score of 93.8%.

Table 3: Evaluation of GRU

Parameters	Value (%)
Accuracy	93.9
Precision	94
Recall	93.9
F1-score	93.8

4.3 Results of Hybrid Model

Fig. 8 illustrates the training and validation accuracy of a hybrid model (Bi-LSTM- GRU) over 25 epochs.



Figure 8: Accuracy of Hybrid Model

At the beginning (Epoch 1), the training accuracy is slightly above 0.86.

It rapidly improves, reaching around 0.90 at the 5th epoch. The accuracy then continues to gradually increase, stabilizing around 0.93 toward the 20th epoch, with minor fluctuations. The final training accuracy at epoch 25 is slightly below 0.93. Starting at a value similar to the training accuracy (0.88), the validation accuracy also increases, but its progress is less steady. It shows more fluctuations compared to the training accuracy, with noticeable peaks and dips. Around epoch 15, a sharp increase is observed, followed by a drop and subsequent stabilization. The final validation accuracy is about 0.93, matching the training accuracy.

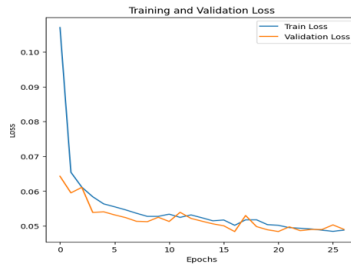


Figure 9: Loss of Hybrid Model

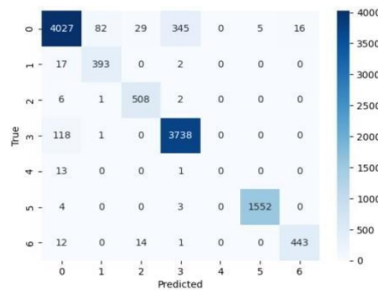


Figure 10: Confusion Matrix of Hybrid Model

Figure 9 shows the loss during training and validation of a hybrid model over an interval of 25 epochs. The training loss is quite significant at around 0.11 at epoch 1, indicating that the model's predictions are detached from the predicted values. It rapidly decreases in the first few epochs, reaching around 0.07 by epoch 5. The loss continues to decline gradually as the epochs progress, stabilizing at around 0.03-0.04 after about 15 epochs. The validation loss also begins relatively high, similar to the training loss, but it

quickly decreases and follows a similar trend. By the 5th epoch, it stabilizes around 0.05, with slight fluctuations but staying below the training loss in many parts of the plot. The overall stability in the validation loss suggests that the model is not over fitting and is generalizing well to unseen data. Both training and validation loss values converge and decrease steadily, representative that the model is learning effectively over time. Figure 10 show the confusion matrix of hybrid model.

Table 4: Evaluation of the Hybrid Model

Parameters	Value (%)
Accuracy	97.07
Precision	94.13
Recall	94.07
F1-score	94

Table 4 provides the evaluation results of the proposed hybrid model, which achieved an Accuracy of 97.07%, Precision of 94.13%, Recall of 94.07%, and an F1-score of 94%.

4.4 Comparative Analysis

The study demonstrates significant advancements in CAD detection, with the hybrid Bi-LSTM+GRU model achieving higher accuracy, precision, recall, and F1 scores compared to existing methods which is demonstrated in Table 5.

Table 5: Evaluation of existing models compared to the proposed model

Author (Year) [Reference]	Methodology	Accuracy (%)
Tang et al., (2023) [38]	CNN	70
Sapra et al., (2023) [39]	DNN	95.2
Choi et al., (2023) [40]	Ob-CAD	63.8
Our Work	Hybrid Model	97.07

The proposed model performs better than previous approaches, achieving an Accuracy of 94.07%, Precision of 94.13%, Recall of 94.07%, and an F1-score of 94%. The graphical representation of the comparison results is illustrated in Fig 11.

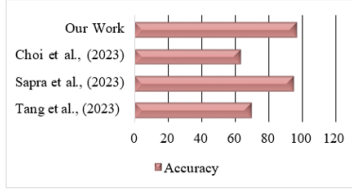


Figure 11: Comparison of previous work v/s present work

The integration of non-invasive data sources reduces patient risks and costs, enabling timely and accurate diagnosis. This approach has the potential to significantly improve clinical decision-making, reducing dependency on invasive diagnostics and accelerating personalized treatment strategies. Machine learning revolutionizes CAD diagnosis by enabling robust analysis of large and complex datasets, identifying patterns and risk factors that traditional methods might miss. Advanced ML models like Bi-LSTM and GRU process temporal and sequential data effectively, making them ideal for analyzing clinical trends and imaging data. The scalability and adaptability of ML techniques make them indispensable for early detection and monitoring of CAD, fostering preventive care, and improving patient outcomes globally.

5 Conclusion

CAD is one of the leading causes of mortality worldwide, necessitating improved diagnostic techniques. Traditional diagnostic methods, such as angiography and stress tests, are often invasive, expensive, or time-consuming. In recent years, the application of ML has emerged as a promising approach for enhancing CAD detection. This paper investigates the various applications of ML algorithms and techniques that can improve the accuracy and efficiency of CAD diagnosis. Machine learning models can identify patterns indicative of CAD with higher precision by analyzing patient data, including clinical records, imaging, and biomarkers. Key models, including Bi-LSTM, GRU, and hybrid models, are used for the detection of CAD on the 3D CCTA dataset. The experimental results show that the hybrid model achieved an accuracy of 97.07%. The findings suggest that machine learning can significantly enhance CAD detection, leading to better patient outcomes through timely intervention and personalized treatment strategies.

References

- [1] A. Abdolmanafi et al. Characterization of coronary artery pathological formations from oct imaging using deep learning. *Biomedical Optics Express*, 9(10):4936–4960, 2018.
- [2] H. A. Ahmed, A. Hameed, and N. Z. Bawany. Network intrusion detection using oversampling technique and machine learning algorithms. *PeerJ Computer Science*, 8:e820, 2022.
- [3] A. F. AlOthman, A. R. W. Sait, and T. A. Alhussain. Detecting coronary artery disease from computed tomography images using a deep learning technique. *Diagnostics*, 12(9):2073, 2022.
- [4] S. Asif et al. Improving the accuracy of diagnosing and predicting coronary heart disease using ensemble method and feature selection techniques. *Cluster Computing*, 27(2):1927–1946, 2024.
- [5] J. Betancur et al. Deep learning analysis of upright-supine high-efficiency spect myocardial perfusion imaging for prediction of obstructive coronary artery disease: A multicenter study. *Journal of Nuclear Medicine*, 60(5):664–670, 2019.
- [6] A. Bibi et al. A hypertuned lightweight and scalable lstm model for hybrid network intrusion detection. *Technologies*, 11(5):121, 2023.
- [7] D. Chicco. Siamese neural networks: An overview. In *Artificial Neural Networks*, pages 73–94. 2021.
- [8] S. H. Choi et al. Electrocardiogram-based deep learning algorithm for screening obstructive coronary artery disease. *BMC Cardiovascular Disorders*, 23(1):287, 2023.
- [9] K. N. Devi, S. Suruthi, and S. Shanthi. Coronary artery disease prediction using machine learning techniques. In *Proceedings of the 8th International Conference on Advanced Computing and Communication Systems (ICACCS)*, pages 1029–1034. IEEE, 2022.
- [10] P. Dileep et al. Automatic heart disease prediction using cluster-based bilstm. *Neural Computing and Applications*, 35(10):7253–7266, 2023.
- [11] M. Duan et al. Machine learning aided non-invasive diagnosis of coronary heart disease based on tongue features fusion. *Technology and Health Care*, pages 1–17, 2024.

- [12] M. R. Dweck et al. Imaging of coronary atherosclerosis—evolution towards new treatment strategies. *Nature Reviews Cardiology*, 13(9):533–548, 2016.
- [13] H. R. Fazlali et al. Vessel segmentation and catheter detection in x-ray angiograms using superpixels. *Medical and Biological Engineering and Computing*, 56:1515–1530, 2018.
- [14] N. Gajbhiye and K. K. Singh. Meta heuristic based optimized intelligent framework for kidney disease detection using deep learning. In *OPJU International Technology Conference*, 2025.
- [15] N. Gajbhiye and K. K. Singh. An optimized depression detection technique using behavioral analysis and machine learning. In *Proceedings of the 6th International Conference on Recent Advances in Information Technology*, 2025.
- [16] N. Gajbhiye, K. K. Singh, and G. S. Mishra. Enhancing crop disease detection systems with explainable ai techniques. In *International Conference on Deep Learning, Artificial Intelligence and Robotics*, 2025.
- [17] S. Gao, Y. Zheng, and X. Guo. Gru-based heart sound analysis for heart failure screening. *Biomedical Engineering Online*, 19:1–17, 2020.
- [18] A. Garavand et al. Efficient model for coronary artery disease diagnosis: A comparative study. *Journal of Healthcare Engineering*, 2022:5359540, 2022.
- [19] A. Hammoud et al. Coronary heart disease prediction: A comparative study of machine learning algorithms. *Journal of Advanced Information Technology*, 15:27–32, 2024.
- [20] Y. Hong et al. Deep learning-based stenosis quantification from coronary ct angiography. In *Medical Imaging: Image Processing*, volume 10949, pages 643–651. SPIE, 2019.
- [21] Y. Huang et al. Using a machine learning-based risk prediction model to analyze coronary artery calcification score. *Computers in Biology and Medicine*, 151:106297, 2022.
- [22] S. Karthikeyini et al. Heart disease prognosis using d-gru with optimization in iomt. *Information Technology and Control*, 52(2):367–380, 2023.

- [23] Q. Li et al. Machine learning in nephrology: Scratching the surface. *Chinese Medical Journal*, 133(6):687–698, 2020.
- [24] L. Lin et al. Machine learning-based models for prediction of the risk of stroke in coronary artery disease patients receiving coronary revascularization. *PLoS One*, 19(2):e0296402, 2024.
- [25] S. Lin et al. Feasibility of using deep learning to detect coronary artery disease based on facial photo. *European Heart Journal*, 41(46):4400–4411, 2020.
- [26] H. Ling et al. Machine learning in diagnosis of coronary artery disease. *Chinese Medical Journal*, 134(4):401–403, 2021.
- [27] C.-Y. Ma et al. Predicting coronary heart disease in chinese diabetics using machine learning. *Computers in Biology and Medicine*, 169:107952, 2024.
- [28] A. Maleki et al. Prevalence of coronary artery disease and the associated risk factors in the adult population of borujerd city, iran. *Journal of Tehran University Heart Center*, 14(1):1–6, 2019.
- [29] M. Mijwil, A. K. Faieq, and M. Aljanabi. Early detection of cardiovascular disease utilizing machine learning techniques. *Iraqi Journal of Computer Science and Mathematics*, 5(1):263–276, 2024.
- [30] A. N. Nowbar et al. Mortality from ischemic heart disease: Analysis of data from the world health organization and coronary artery disease risk factors. *Circulation: Cardiovascular Quality and Outcomes*, 12(6):e005375, 2019.
- [31] A. Ogunpola et al. Machine learning-based predictive models for detection of cardiovascular diseases. *Diagnostics*, 14(2):144, 2024.
- [32] M. Popov et al. Dataset for automatic region-based coronary artery disease diagnostics using x-ray angiography images. *Scientific Data*, 11(1):20, 2024.
- [33] F. Rangraz Jeddi et al. Machine learning approaches for detecting coronary artery disease using angiography imaging: A scoping review. In *Healthcare Transformation with Informatics and Artificial Intelligence*, pages 244–248. 2023.

- [34] D. D. Reddy and G. H. Bindu. Feature selection model-based intrusion detection system for cyberattacks on the internet of vehicles using cat and mouse optimizer. 2024.
- [35] V. Sapra et al. Integrated approach using deep neural network and cbr for detecting severity of coronary artery disease. *Alexandria Engineering Journal*, 68:709–720, 2023.
- [36] P. K. Shrivastava, M. Sharma, and A. Kumar. Hcbilstm: A hybrid model for predicting heart disease. *Measurement: Sensors*, 25:100657, 2023.
- [37] K. K. Singh, N. Gajbhiye, and G. S. Mishra. Exploring multi-stage deep convolutional neural network for medicinal plant disease diagnosis. In *International Conference on Deep Learning, Artificial Intelligence and Robotics*, 2025.
- [38] P. Tang et al. Early detection of coronary artery disease using deep learning-based electrocardiography. *Aging*, 15(9):3524–3535, 2023.
- [39] M. G. Veerabaku et al. Intelligent bi-lstm with architecture optimization for heart disease prediction. *Biomedicines*, 11(4):1167, 2023.
- [40] N. A. Vinay et al. An rnn-bilstm based multi-decision gan approach for recognition of cardiovascular disease. *IEEE Access*, 2024.
- [41] Y. Xiao et al. An intrusion detection model based on feature reduction and convolutional neural networks. *IEEE Access*, 7:42210–42219, 2019.
- [42] R. Yilmaz and F. H. Yagin. Early detection of coronary heart disease based on machine learning methods. *Medical Records*, 4(1):1–6, 2022.
- [43] A. Zeng et al. Imagecas: A large-scale dataset and benchmark for coronary artery segmentation. *Computerized Medical Imaging and Graphics*, 109:102287, 2023.
- [44] M. Zreik et al. Deep learning analysis of the myocardium in coronary ct angiography for identification of patients with functionally significant coronary artery stenosis. *Medical Image Analysis*, 44:72–85, 2018.